Available online at www.sciencedirect.com
SCIENCE DIRECT®
Physica A 351 (2005) 211–226
PHYSICA A
www.elsevier.com/locate/physa

Coordinated collective motion in a motile particle group with a leader

Shumei Mu , Tianguang Chu*, Long Wang

Intelligent Control Laboratory, Department of Mechanics and Engineering Science, Peking University, Beijing 100871, PR China

Received 10 November 2004
Available online 25 January 2005

Abstract

We study the collective dynamics of a group of motile particles with a leader. The leader is unaffected by the particle members whereas each member is influenced by the leader and the other members. By using coupled oscillators theory and Lyapunov function method, we show how the group dynamics depends on the motion of the leader and the coupling weights among all particles. Generally speaking, two types of collective motions will occur, depending on different ranges of the coupling weights among the member particles. One is that all the member particles will move in the same direction and the other is that all the member particles move in such a way that the weighted centroid of the group approaches a fixed position. In each case, all the member particles eventually move in the same manner except for the directions of the motion in certain cases. Numerical simulations are worked out to demonstrate the theoretical results. The study suggests potential approaches to control a group motion by steering the motion of the leader and adjusting coupling patterns. This is of practical interest in applications of multiagent systems.

PACS: 05.45.−a; 05.65.+b; 45.50.−j; 87.18.Ed

Keywords: Collective motion; Coupled phase oscillators; Multiagent systems; Networked systems; *V*-function

*Corresponding author.
E-mail addresses: mushumei@pku.edu.cn (S. Mu), chutg@pku.edu.cn (T. Chu).

0378-4371/$ - see front matter © 2005 Elsevier B.V. All rights reserved.
doi:10.1016/j.physa.2004.12.054

1. Introduction

In recent years, collective motion and self-organized behavior of swarms, agents, and particles have become a major objective in many fields such as ecology and theoretical biology [1,2], biological physics [3–12], and control engineering [13–17]. The studies focus on understanding the general mechanisms and operational principles of such coordinated cooperative phenomena as well as their potential applications in various engineering practice such as control of multi-robots and traffic flows, etc. For example, the authors of Ref. [3] proposed a simple model for phase transition of a group of self-driven particles and numerically demonstrated complex dynamics of the model. A subsequent analysis of a continuum model was presented in Ref. [5]. Collective behavior of self-propelled particles was also investigated in Refs. [7,8]. Crawford and Davies [6] and Acebrón and Spigler [9] studied synchronization of globally coupled oscillators. An interesting issue that arises in the studies is the collective behavior of particle groups with leaders. For instance, in Ref. [13], moving reference points were viewed as virtual leaders used to manipulate the geometry of autonomous vehicle group and direct the motion of group. The cohesion of the members of swarms following an edge-leader was analyzed in Ref. [14]. Jadbabaie et al. [15] investigated leaderless/leader coordination of mobile autonomous agents using nearest neighbor rules. Leader–follower networks were also considered in Ref. [18].

In a recent paper [19], the collective motion of a self-propelled particle group has been analyzed by viewing the particle group as a coupled phase oscillator system. It was shown that under sufficiently large coupling strength, the particles either move in parallel or maintain the centroid of the particle group motionless eventually. It also presented formation control design. However, the model of Ref. [19] did not consider the role of a leader in the particle group.

In this paper we investigate the dynamics of a coupled particle group with an independent leader. We show that the leader's dynamics can significantly influence the collective motion of particle group. The evolution of the particle members will eventually be the same as that of the leader for certain ranges of the coupling weights. This makes it possible to control the particle group by steering the motion of the leader, which is of practical interest in applications such as control of multi-robots or autonomous vehicles.

The paper is organized as follows. Section 2 presents the particle model. Dynamics analysis of the model is carried out in Section 3. Section 4 gives numerical simulations of the theoretical results. Some conclusions are drawn in Section 5.

By convention, $\mathbb{R}$ represents the real number set. The notation $\theta_0 \to \theta_0^*(+)$ means $\theta_0 > \theta_0^*$ and $\theta_0 \to \theta_0^*$, and $\theta_0 \to \theta_0^*(-)$ denotes $\theta_0 < \theta_0^*$ and $\theta_0 \to \theta_0^*$.

2. Particle model

We consider a group of $(N+1)$ identical particles (of unit mass) moving in the plane at unit speed, in which a particle indexed by 0 is assigned as the "leader" and

the other particles indexed by $1,\ldots,N$ are referred to as "members". The leader is unaffected by the members whereas each member is influenced by the leader and the other members. A continuous-time kinematic model of the $(N+1)$ particles is described as follows:

$$\begin{aligned}
\dot{r_0} &= \mathrm{e}^{\mathrm{i}\theta_0}\,,\\
\dot{\theta_0} &= F(\theta_0)\,,\\
\dot{r_k} &= \mathrm{e}^{\mathrm{i}\theta_k}\,,\\
\dot{\theta_k} &= K_0\,\sin(\theta_0-\theta_k)+K_1\sum_{j=1}^{N}\sin(\theta_j-\theta_k)\,,
\end{aligned}\tag{1}$$

where $1\leqslant k\leqslant N$. In complex notation, the vector $r_k\in\mathbb{C}\approx\mathbb{R}^2$ (the punctured complex plane) denotes the position of particle k and the angle θ_k denotes the direction of its (unit) velocity vector $\mathrm{e}^{\mathrm{i}\theta_k}=\cos\theta_k+\mathrm{i}\sin\theta_k, 0\leqslant k\leqslant N$. $F(\theta_0)$ is a smooth function defined in $I\subseteq\mathbb{R}$. When $F(\theta_0)$ is not identical with 0, we assume that the equilibrium points of $\dot{\theta_0}=F(\theta_0)$ (if any) are all hyperbolic and that the motion of the leader has not finite escape time. $K_0,K_1\in\mathbb{R}$ are two parameters with $0<K_0/K_1<N$, specifying the coupling strength between each member and the leader and the coupling strength between any two members, respectively. The initial values of all θ_k and r_k are selected arbitrarily.

Collective dynamics of Eqs. (1) without variables r_0,θ_0 (and hence $K_0=0$) has been studied in Refs. [19,20]. In the present form, since θ_0 is independent of all θ_k whereas each θ_k depends on θ_0 for $k=1,\ldots,N$, the dynamics of θ_k are in general more complex than that concerned before. In the following we will analyze the dynamics of model (1) by using coupled oscillators theory [20].

3. Dynamics analysis

Observe that the right side of Eqs. (1) does not depend on the position variable r (here we omit the index) and r are dependent on θ. Hence we only need to analyze the dynamics of θ in the sequel and then examine the dynamics of r when needed. For convenience, denote $\bar{\theta}_k=\theta_k-\theta_0, k=0,1,\ldots,N$. For $k=1,\ldots,N$, the dynamics of $\bar{\theta}_k$ are described as follows:

$$\dot{\bar{\theta}}_k=-\left(K_0+K_1\sum_{j=1}^{N}\cos\bar{\theta}_j\right)\sin\bar{\theta}_k+K_1\left(\sum_{j=1}^{N}\sin\bar{\theta}_j\right)\cos\bar{\theta}_k-F(\theta_0)\,.\tag{2}$$

Notice that Eq. (2) is similar to the general reducible phase oscillator model in Ref. [20], where the authors presented a reduction process and analyzed the dynamics of the model using Lyapunov second method. Their method and results have also been used in Ref. [19]. Similar to the arguments of Watanabe

and Strogatz [20], we can analyze the dynamics of $\bar{\theta}_k$. We will make use of the following notations:

$$\bar{g} = \frac{1}{N}\sum_{j=1}^{N} \cos\,\bar{\theta}_j\,,$$

$$\bar{h} = \frac{1}{N}\sum_{j=1}^{N} \sin\,\bar{\theta}_j\,,$$

$$P_{\bar{\theta}} = \frac{1}{N+1}\left(K_0 e^{i\bar{\theta}_0} + K_1 \sum_{j=1}^{N} e^{i\bar{\theta}_j}\right)$$

$$= \frac{1}{N+1}(K_0 + K_1 N\bar{g} + iK_1 N\bar{h})\,,$$

$$R = \frac{1}{N+1}\left(K_0 r_0 + K_1 \sum_{k=1}^{N} r_k\right). \tag{3}$$

Clearly, R is the position vector of the weighted centroid of the group. One has

$$\dot{R} = P_{\bar{\theta}} e^{i\theta_0}\,.$$

For convenience in the following discussion, we rewrite the equation of θ_0 in Eqs. (1) as

$$\dot{\theta}_0 = F(\theta_0)\,. \tag{4}$$

To investigate the dynamics of $\bar{\theta}_k$, we need first to determine qualitative properties of θ_0. Without loss of generality, we assume that $F(\theta_0) \not\equiv 0$. Then by assumption the equilibrium points of Eq. (4) (if any) are all hyperbolic. Hence for any initial value $\theta_0(t_0)$ in I, the evolution of θ_0 has one of the following properties, depending on properties of $F(\theta_0)$ and $\theta_0(t_0)$:

*P*1. θ_0 *monotonically tends to an equilibrium point of Eq.* (4);
*P*2. θ_0 *monotonically increases and approaches the boundary of* I;
*P*3. θ_0 *monotonically decreases and approaches the boundary of* I.

In the last two cases the sign of $F(\theta_0)$ does not change in I. In the first case there exists at least one equilibrium point of Eq. (4) in I and according to the assumption on $F(\theta_0)$, the equilibrium point is either stable or unstable. This implies that as $t \to +\infty$, θ_0 either monotonically tends to the equilibrium point or monotonically approaches the boundary of I. We summarize these properties in the following four cases, where θ_0^* is an equilibrium point of Eq. (4):

- $\theta_0 \in P1(+)$ denotes that $P1$ occurs and $\theta_0 \to \theta_0^*(+)$ as $t \to +\infty$.
- $\theta_0 \in P1(-)$ denotes that $P1$ occurs and $\theta_0 \to \theta_0^*(-)$ as $t \to +\infty$.

- $\theta_0 \in P2$ denotes that $P2$ occurs.
- $\theta_0 \in P3$ denotes that $P3$ occurs.

From this, we have the following lemma.

Lemma 1. *For any initial value $\theta_0(t_0) \in I$, the sign of $F(\theta_0)$ is eventually constant as $t \to +\infty$. Specifically, $F(\theta_0)>0$ for $\theta_0 \in P1(-)$ or $\theta_0 \in P2$, and $F(\theta_0)<0$ for $\theta_0 \in P1(+)$ or $\theta_0 \in P3$.*

Lemma 1 will be useful in analysis of the dynamics of $\bar{\theta}_k$. Observe that Eq. (2) includes a term $-K_0 \sin \bar{\theta}_k - F(\theta_0)$ in its right-hand side, which comes from the influence of the leader on every particle member, so the governing equations of $\bar{\theta}_k$ are different from that considered in Refs. [19,20]. We will investigate the dynamics of $\bar{\theta}_k$ by taking a coordinate transformation and analyzing the dynamics of new variables.

3.1. Change of variables

From Eqs. (3), we have

$$\sum_{j=1}^{N} \cos \bar{\theta}_j = N\bar{g}, \quad \sum_{j=1}^{N} \sin \bar{\theta}_j = N\bar{h}\,.$$

Inserting them into Eq. (2) yields

$$\dot{\bar{\theta}}_k = NK_1\bar{h} \cos \bar{\theta}_k - (K_0 + NK_1\bar{g}) \sin \bar{\theta}_k - F(\theta_0) \tag{5}$$

for $k = 1, \ldots, N$. Take the changes of variables [20]

$$\tan\left[\frac{1}{2}(\bar{\theta}_k - \Theta)\right] = \sqrt{\frac{1+\gamma}{1-\gamma}} \tan\left[\frac{1}{2}(\psi_k - \Psi)\right] \tag{6}$$

for $k = 1, \ldots, N$, which map N-dimensional state vector $(\bar{\theta}_1, \bar{\theta}_2, \ldots, \bar{\theta}_N)$ to the $(N+3)$-dimensional state vector $(\gamma, \Theta, \Psi, \psi_1, \ldots, \psi_N)$. In Eq. (6), Θ and Ψ are two rigid rotation variables, γ is a dilation with $0 \leqslant \gamma < 1$, and ψ_k, $k = 1, \ldots, N$ are new phase variables. All these variables depend on time. Eq. (6) may be regarded as a way to redistribute the phase variables $\bar{\theta}_k$ on unit circle, for more detailed implication about the transformation we refer to Ref. [20].

From Eq. (6) and certain trigonometric identities, one can get two useful formulas:

$$\sin(\bar{\theta}_k - \Theta) = \frac{\sqrt{1-\gamma^2}\,\sin(\psi_k - \Psi)}{1 - \gamma\cos(\psi_k - \Psi)}, \quad \cos(\bar{\theta}_k - \Theta) = \frac{\cos(\psi_k - \Psi) - \gamma}{1 - \gamma\cos(\psi_k - \Psi)}\,. \tag{7}$$

Differentiating Eq. (6) with respect to time, using some trigonometric identities and after some algebraic manipulations, we get

$$\frac{\dot{\bar{\theta}}_k - \dot{\Theta}}{1+\cos(\bar{\theta}_k - \Theta)} = \frac{1}{1-\gamma}\frac{\dot{\gamma}}{\sqrt{1-\gamma^2}}\frac{\sin(\psi_k - \Psi)}{1+\cos(\psi_k - \Psi)} + \sqrt{\frac{1+\gamma}{1-\gamma}}\frac{\dot{\psi}_k - \dot{\Psi}}{1+\cos(\psi_k - \Psi)} . \tag{8}$$

Inserting Eqs. (5) and (7) into Eq. (8) and after some algebraic manipulations, we obtain

$$0 = [K_1 N\bar{h}\cos\bar{\theta}_k - (K_0 + K_1 N\bar{g})\sin\bar{\theta}_k - F(\theta_0) - \dot{\Theta}] \times[1-\gamma\cos(\psi_k - \Psi)] - \frac{\dot{\gamma}\sin(\psi_k - \Psi)}{\sqrt{1-\gamma^2}} - \sqrt{1-\gamma^2}(\dot{\psi}_k - \dot{\Psi}) . \tag{9}$$

Note that

$$\begin{aligned} \cos\bar{\theta}_k &= \cos(\bar{\theta}_k - \Theta)\cos\Theta - \sin(\bar{\theta}_k - \Theta)\sin\Theta , \\ \sin\bar{\theta}_k &= \sin(\bar{\theta}_k - \Theta)\cos\Theta + \cos(\bar{\theta}_k - \Theta)\sin\Theta . \end{aligned} \tag{10}$$

Substituting Eqs. (10) into Eq. (9) and using Eqs. (7), we have

$$\begin{aligned} 0 = & -\sqrt{1-\gamma^2}\dot{\psi}_k \\ & + [K_1 P - K_0\sin\Theta + \gamma(F(\theta_0) + \dot{\Theta})]\cos(\psi_k - \Psi) \\ & - \left[(K_1 Q + K_0\cos\Theta)\sqrt{1-\gamma^2} + \frac{\dot{\gamma}}{\sqrt{1-\gamma^2}}\right]\sin(\psi_k - \Psi) \\ & + [(-K_1 P + K_0\sin\Theta)\gamma - (F(\theta_0) + \dot{\Theta}) + \sqrt{1-\gamma^2}\dot{\Psi}] \end{aligned} \tag{11}$$

for $k = 1, \ldots, N$ and

$$\begin{aligned} P &= N(\bar{h}\cos\Theta - \bar{g}\sin\Theta) = \sum_{j=1}^{N}\frac{\sqrt{1-\gamma^2}\sin(\psi_j - \Psi)}{1-\gamma\cos(\psi_j - \Psi)} , \\ Q &= N(\bar{h}\sin\Theta + \bar{g}\cos\Theta) = \sum_{j=1}^{N}\frac{\cos(\psi_j - \Psi) - \gamma}{1-\gamma\cos(\psi_j - \Psi)} . \end{aligned} \tag{12}$$

Observe that if we set in Eq. (11) that

$$\begin{aligned} & K_1 P - K_0\sin\Theta + \gamma(F(\theta_0) + \dot{\Theta}) = 0 , \\ & (K_1 Q + K_0\cos\Theta)\sqrt{1-\gamma^2} + \frac{\dot{\gamma}}{\sqrt{1-\gamma^2}} = 0 , \\ & (-K_1 P + K_0\sin\Theta)\gamma - (F(\theta_0) + \dot{\Theta}) + \sqrt{1-\gamma^2}\dot{\Psi} = 0 , \end{aligned}$$

i.e., let the three variables (γ, Θ, Ψ) satisfy the following differential equations:

$$\begin{aligned}
&\dot{\gamma} = -(1-\gamma^2)(K_1 Q + K_0 \cos\Theta)\,,\\
&\gamma\dot{\Psi} = -\sqrt{1-\gamma^2}(K_1 P - K_0 \sin\Theta)\,,\\
&\gamma\dot{\Theta} = -K_1 P + K_0 \sin\Theta - \gamma F(\theta_0)
\end{aligned} \tag{13}$$

for $\gamma \neq 0$ and

$$\begin{aligned}
&0 = K_1 \sum_{j=1}^{N} \sin(\psi_j - \Psi) - K_0 \sin\Theta\,,\\
&\dot{\gamma} = -K_1 \sum_{j=1}^{N} \cos(\psi_j - \Psi) - K_0 \cos\Theta\,,\\
&0 = -\dot{\theta}_0 - \dot{\Theta} + \dot{\Psi}
\end{aligned} \tag{14}$$

for $\gamma = 0$, where θ_0 satisfies Eq. (4), then Eq. (11) reduces to

$$\dot{\psi}_k = 0, \quad k = 1, \ldots, N\,. \tag{15}$$

Thus the dynamics analysis of $\bar{\theta}_k$ is converted into that of γ, Θ, Ψ, and ψ_k governed by Eqs. (4), (13), (14), and (15).

Eq. (15) means that the N new phase variables ψ_k are frozen. Hence ψ_k can be considered as parameters. Under the coordinate transformation (6) the original N variables are converted into 3 new variables and N parameters. Hence three constraints can be imposed on the initial values of γ, Θ, Ψ and ψ_k, $k = 1, \ldots, N$. Here we impose the constraints

$$\sum_{k=1}^{N} \cos\psi_k = \frac{K_0}{K_1}, \quad \sum_{k=1}^{N} \sin\psi_k = 0 \tag{16}$$

on the initial values of ψ_k and hence on ψ_k for $k = 1, \ldots, N$.

Under constraints (16), it yields from the first equation in Eqs. (14) that

$$\sin\Psi + \sin\Theta = 0\,. \tag{17}$$

From this we further have

$$\cos\Psi + \cos\Theta = 0 \quad \text{or} \quad \cos\Psi - \cos\Theta = 0\,.$$

And we impose a constraint on the initial values of Θ and Ψ such that

$$\cos\Psi + \cos\Theta = 0 \quad \text{for } \gamma = 0\,. \tag{18}$$

Thus from the second equation of Eqs. (14) we get

$$\dot{\gamma} = 0 \quad \text{for } \gamma = 0\,.$$

Again from Eqs. (14) we see that for $\gamma = 0$, $(\theta_0, \gamma, \Theta, \Psi)$ evolves on a manifold defined by

$$M = \{(\theta_0, \gamma, \Theta, \Psi) : \gamma = 0,\ \Psi - \Theta - \theta_0 = C\}\,, \tag{19}$$

where θ_0 satisfies Eq. (4) and C is a constant.

In the following we will analyze the dynamics of Θ, Ψ and γ governed by Eqs. (4) and (13) with N parameters ψ_k and constraints (16) and (18) by introducing an auxiliary V function. From the analysis we finally obtain the dynamics of θ_k.

3.2. V-function and convergent dynamics

Observe that Θ is coupled with Ψ, γ and θ_0, we choose a V-function as follows:

$$V = \sum_{k=1}^{N} \ln\left(\frac{1-\gamma\cos(\psi_k-\Psi)}{\sqrt{1-\gamma^2}}\right) - \frac{K_0}{K_1}\gamma(1+\cos\Theta) - \frac{K_0}{K_1}(\ln(1-\gamma)-v)\,, \tag{20}$$

where if $F(\theta_0)\equiv 0$, then $v=0$; otherwise, for $K_1>0$

$$v = \begin{cases} 2\theta_0 & \text{if } \theta_0 \in P2\,, \\ -2\theta_0 & \text{if } \theta_0 \in P3\,, \\ \frac{1}{2}(\theta_0-\theta_0^*-2)^2 & \text{if } \theta_0 \in P1(+)\,, \\ \frac{1}{2}(\theta_0-\theta_0^*+2)^2 & \text{if } \theta_0 \in P1(-) \end{cases} \tag{21}$$

and for $K_1<0$,

$$v = \begin{cases} -2\theta_0 & \text{if } \theta_0 \in P2\,, \\ 2\theta_0 & \text{if } \theta_0 \in P3\,, \\ \frac{1}{2}(\theta_0-\theta_0^*+2)^2 & \text{if } \theta_0 \in P1(+)\,, \\ \frac{1}{2}(\theta_0-\theta_0^*-2)^2 & \text{if } \theta_0 \in P1(-) \end{cases} \tag{22}$$

with θ_0 being the solution of Eq. (4) and θ_0^* an equilibrium point of it.

Below we analyze the dynamics of Eqs. (13) and (4) using the derivatives of the V-function with respect to time t and to γ, respectively. Differentiating V with respect to t, making use of Eqs. (12) and (13), and after some algebraic manipulations, we have

$$\dot{V} = K_1 G_1 G_2 + K_1 G_3 + (K_0/K_1) G_4\,, \tag{23}$$

where

$$G_1 = \sum_{k=1}^{N} \frac{\gamma-\cos(\psi_k-\Psi)}{1-\gamma\cos(\psi_k-\Psi)} + \frac{K_0}{K_1}(1+\gamma) - \frac{K_0}{K_1}(1-\gamma^2)(1+\cos\Theta)\,,$$

$$G_2 = \sum_{k=1}^{N} \frac{\gamma-\cos(\psi_k-\Psi)}{1-\gamma\cos(\psi_k-\Psi)} - \frac{K_0}{K_1}\cos\Theta\,,$$

$$G_3 = \left(\sum_{k=1}^{N} \frac{\sqrt{1-\gamma^2}\,\sin(\psi_k-\Psi)}{1-\gamma\cos(\psi_k-\Psi)} - \frac{K_0}{K_1}\sin\Theta\right)^2,$$

$$G_4 = \dot{v} - \gamma\sin\Theta F(\theta_0)\,.$$

Evidently, $G_3 \geqslant 0$ for all $(\gamma, \Theta, \Psi, \theta_0)$ and $G_4 = 0$ if $F(\theta_0) \equiv 0$. We make the following assertion.

Assertion. *For all* $(\gamma, \Theta, \Psi, \theta_0)$

(i) $G_1 \geqslant 0$, $G_2 \geqslant 0$ *and* $G_1 = 0$ *if and only if* $\gamma = 0$;
(ii) *if* $F(\theta_0) \not\equiv 0$, *then* $G_4 > 0$ (*resp.* $G_4 < 0$) *for* $K_1 > 0$ (*resp.* $K_1 < 0$) *as* t *is large enough.*

The proof of the assertion is presented in Appendix A. From this it follows that $K_1 \dot{V} > 0$ for all $(\gamma, \Theta, \Psi, \theta_0)$ as t is large enough. This implies that V eventually increases along the solutions of Eqs. (4) and (13) for $K_1 > 0$ and decreases for $K_1 < 0$. On the other hand, by differentiating V-function with respect to γ, we obtain

$$\frac{\partial V}{\partial \gamma} = \frac{G_1}{1-\gamma^2} > 0$$

for $0 < \gamma < 1$. This implies that V strictly increases with γ and vice versa. Thus along the solutions of Eqs. (4) and (13),

- if $K_1 > 0$, then $\gamma \to 1$;
- if $K_1 < 0$, then $\gamma \to 0$.

Hence the dynamics of Eqs. (13) depends on the sign of K_1. We consider two cases in the following.

First, for the case of $K_1 > 0$, i.e., $\gamma \to 1$, we have from Eqs. (7),

$$\bar{\theta}_k \to \Theta \pm \pi, \quad \text{i.e., } \theta_k \to \theta_0 + \Theta + \pi, \quad (\text{mod}(2\pi)) \tag{24}$$

for $k = 1, \ldots, N$, which mean that all phase variables $\bar{\theta}_k$ tend to be synchronizing (this corresponds to the in-phase state of phase oscillators in Ref. [20]). This indicates that all the members will move in the same direction eventually. Also note that the equations for the position of every member are all in the same form. Hence all members will move in the same manner as $t \to +\infty$.

To compare the motion of the members with that of the leader, notice that from Eqs. (1) it follows that

$$\begin{aligned}
\dot{\bar{\theta}}_k &= K_0 \sin(\theta_0 - \theta_k) + K_1 \sum_{j=1}^{N} \sin(\theta_j - \theta_k) - F(\theta_0) \\
&= -K_0 \sin \bar{\theta}_k + K_1 \sum_{j=1}^{N} \sin(\bar{\theta}_j - \Theta - \bar{\theta}_k + \Theta) - F(\theta_0) \\
&= -K_0 \sin \bar{\theta}_k + K_1 \left[\cos(\bar{\theta}_k - \Theta) \sum_{j=1}^{N} \frac{\sqrt{1-\gamma^2} \sin(\psi_j - \Psi)}{1 - \gamma \cos(\psi_j - \Psi)} \right. \\
&\quad \left. - \frac{\sqrt{1-\gamma^2} \sin(\psi_k - \Psi)}{1 - \gamma \cos(\psi_k - \Psi)} \sum_{j=1}^{N} \cos(\bar{\theta}_j - \Theta) \right] - F(\theta_0)
\end{aligned}$$

for $k = 1, 2, \ldots, N$. As $\gamma \to 1$ the above equations approximate to the following form:

$$\dot{\bar{\theta}}_k = -K_0 \sin \bar{\theta}_k - F(\theta_0) . \tag{25}$$

If $F(\theta_0)/K_0$ tends to a constant a along the solution of (4) as $t \to +\infty$ and $|a| \leqslant 1$, then either $-\arcsin a$ or $\pi + \arcsin a \,(\mathrm{mod}(2\pi))$ is a stable equilibrium point of (25). Denote the stable equilibrium point by c_k. It follows that $\bar{\theta}_k \to c_k$, i.e., $\theta_k \to \theta_0 + c_k$ as $t \to +\infty$. Hence the governing equation of r_k approximate to the following form:

$$\dot{r}_k = \dot{r}_0 e^{ic_k}$$

as $t \to +\infty$, where c_k are constants, $k = 1, 2, \ldots, N$. This implies that the members eventually move in the same manner as the leader does if the directions of motion are disregarded.

Next, we consider the case of $K_1 < 0$, i.e., $\gamma \to 0$. From Eqs. (7) we have

$$\sin(\bar{\theta}_k - \Theta) \to \sin(\psi_k - \Psi), \quad \cos(\bar{\theta}_k - \Theta) \to \cos(\psi_k - \Psi)$$

as $\gamma \to 0$. For $\gamma = 0$, i.e., confined to M, the following equalities hold for $k = 1, \ldots, N$

$$\sin(\bar{\theta}_k - \Theta) = \sin(\psi_k - \Psi), \quad \cos(\bar{\theta}_k - \Theta) = \cos(\psi_k - \Psi) . \tag{26}$$

From Eqs. (17), (18) and (26) we have

$$\sin \bar{\theta}_k = \sin(\bar{\theta}_k - \Theta + \Theta) = -\sin \psi_k, \quad \cos \bar{\theta}_k = \cos(\bar{\theta}_k - \Theta + \Theta) = -\cos \psi_k .$$

Summing above equalities from $k = 0$ to N and using constraints (16), we get

$$\sum_{k=1}^{N} \cos \bar{\theta}_k = -\frac{K_0}{K_1}, \quad \sum_{k=1}^{N} \sin \bar{\theta}_k = 0 . \tag{27}$$

It follows that $N\bar{g} = -K_0/K_1, N\bar{h} = 0$, i.e., $P_{\bar{\theta}} = 0$, which is equivalent to constraints (16) restricted on M. Therefore, $P_{\bar{\theta}} \to 0$ as $\gamma \to 0$. This implies that the weighted centroid of the particle group tends to a fixed position as $t \to +\infty$.

As for the motion of each individual member, it follows from Eqs. (26) that

$$\theta_k = \psi_k - C, \quad (\mathrm{mod}(2\pi)) \tag{28}$$

on M for $k = 1, \ldots, N$, where $C = \Psi - \theta_0 - \Theta$. This means that for $k = 1, \ldots, N$, θ_k are constants on M for given parameters ψ_k (this corresponds to the splay state of the phase oscillators in Ref. [20]). Thus all members move along straight lines on the manifold M. So without considering the directions of motion we can say that the members will move in the same manner.

Summarizing the above discussion we arrive at the following conclusion.

Proposition. *Consider the particle model in Eqs.* (1).

1. *If* $K_1 > 0$, *then the members will all move in the same direction eventually.*
2. *If* $K_1 < 0$, *the members will move in such a manner that the weighted centroid of the particle group approaches a fixed point and they move along straight lines as* $t \to +\infty$.

3. *In each case, neglecting the directions of motion, all members will eventually move in the same manner as t is large enough.*
4. *Particularly, in the case of* $K_1>0$, *if* $F(\theta_0)/K_0$ *tends to a constant in* $[-1,1]$ *along solutions of Eq.* (4) *as* $t\to+\infty$, *then all members will eventually move in the same manner as the leader does by neglecting motion directions.*

The results imply that the members will eventually tend to form certain formations.

Remark 1. In above discussion, if we impose constraints

$$\sum_{k=1}^{N}\cos\psi_k=-\frac{K_0}{K_1},\quad \sum_{k=1}^{N}\sin\psi_k=0$$

on ψ_k, $k=1,2,\ldots,N$ instead of Eq. (17), and

$$\cos\Psi-\cos\Theta=0\quad\text{for }\gamma=0\,.$$

on the initial values of Θ and Ψ instead of Eq. (18), we can obtain the same results.

Remark 2. Observe that the condition of $0<K_0/K_1<N$ is only used in the case of $K_1<0$ and is not required for the case of $K_1>0$. Therefore, Proposition (1) and (4) also hold for (1) for $K_1>0$ and $K_0/K_1\geqslant N$.

4. Numerical simulations

To demonstrate the preceding theoretical analysis, we have performed a lot of numerical simulations. Here we display some of them. In the numerical simulations, we choose one leader and ten members. In the figures presented below, the arrows on the curves indicate the directions of the motion. The values of t in the figures indicate the time slots for simulations.

Fig. 1 presents a set of simulation results for position evolutions of eleven particles described by Eqs. (1) with $F(\theta_0)=0.25$ and different values of the pair (K_0,K_1) as indicated in the figures. In Figs. 1(a)–(d), each curve indicates a trajectory of the motion of a particle and the trajectories of the leader are the same as shown in Fig. 1(a). Figs. 1(a) and (b) show the motion of the particles with $K_1>0$ and $K_1<0$, respectively. The trajectories in the similar shapes in each figure show that all the members almost move in the same manner if one neglects the direction of motion. This agrees with the analytical result of Proposition (3). Fig. 1(a) also shows that the members and the leader move in the same manner, as predicted in Proposition (4) because of $F(\theta_0)/K_0\equiv 0.5$ for all t in this case. From Fig. 1(b), it can be seen that the particle members are split into two subgroups whose motions are indicated by the dashed and the solid lines, respectively. The simulations in Figs. 1(b) and (c) are carried out for the same value of (K_0,K_1) and different running time of $t=6\times10^4$ and 1.6×10^4, respectively. Fig. 1(d) is an enlargement of the box at the center of Fig. 1(c), in which we have removed some trajectories for the sake of clarity and only

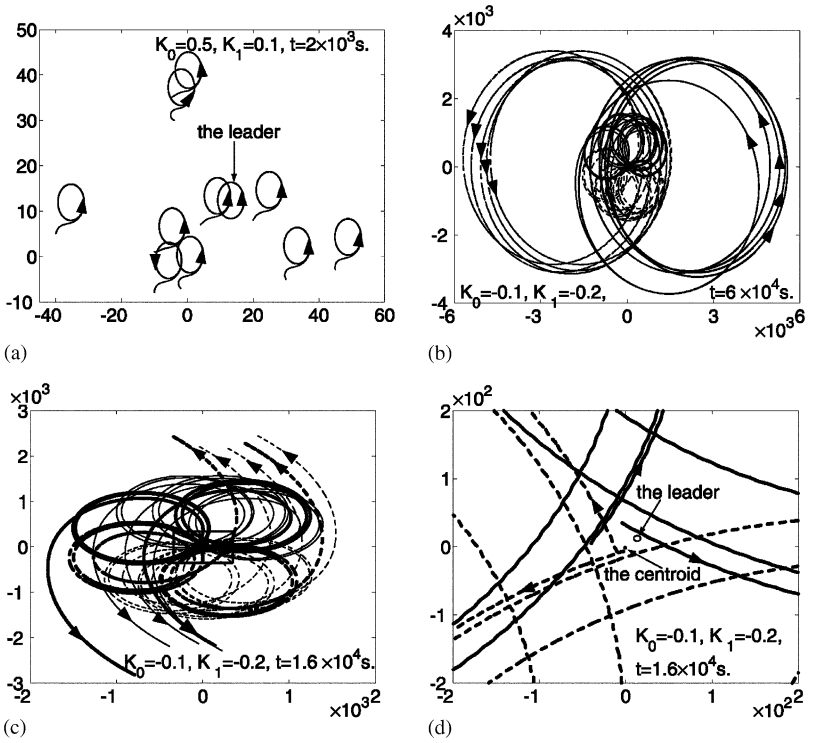

Fig. 1. Phase diagrams of the position dynamics of the particles with $F(\theta_0) = 0.25$ and different values of the pair (K_0, K_1). The abscissa axis and the ordinate axis represent the first and the second components of the position vector r, respectively, in (a)–(d).

left the trajectories of the leader and the weighted centroid, as well as that of 4 members which are arbitrarily chosen and indicated by the thick lines in Fig. 1(c). From Fig. 1(d), we can see that the trajectory of the weighted centroid of the group appears to be a point. This agrees with the analytical result of Proposition (2) that for $K_1 < 0$, the position of the weighted centroid of the group approaches a fixedpoint eventually.

Figs. 2(a)–(c) show the evolutions of the directions of motion of the particles illustrated in Fig. 1. In Fig. 2(a), all θ_k evolve almost along a straight line in time. This indicates that for $K_1 > 0$ the members move in the same direction. Fig. 2(b) is an enlargement of the box in Fig. 2(a), in which a small distance between the two lines shows that there exists a small difference between the directions of the members and the leader. Fig. 2(c) shows the evolutions of the motion directions for $K_1 < 0$. It can be seen that all θ_k evolve almost along two parallel straight lines with a distant of π as $t > 1.3 \times 10^4$. This indicates that the motile particle members are split into two subgroups with each group moving in the same direction while the two groups moving in opposite directions. Also, the segments in Fig. 2(c) for $t < 1.3 \times 10^4$ are

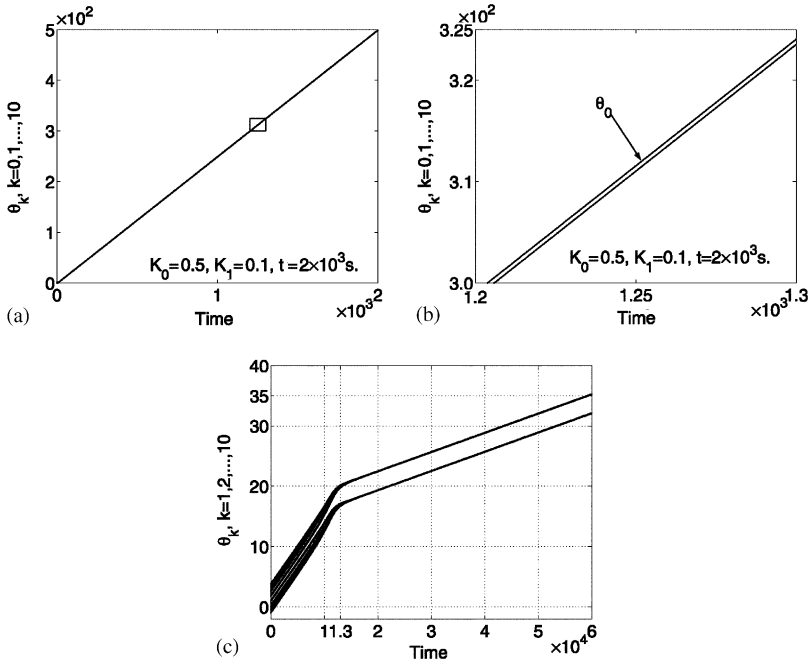

Fig. 2. Evolutions of the directions of the motion of the particles considered in Fig. 1.

almost straight and are steeper than those for $t > 1.3 \times 10^4$. This indicates that the directions of motion of the particles change more slowly as t increases. From Fig. 2(c) it can be evaluated that the slope of the lines for $t > 1.3 \times 10^4$ is about 3.1915×10^{-4}. Thus the change of the direction of motion is very small. This agrees with the analytical result of Proposition (2) that the particle members will eventually move along straight lines as $t \to +\infty$.

Fig. 3 shows another group of simulation results of model (1) with two sets of parameters. Figs. 3(a)–(d) assume that $F(\theta_0) = 0.25$ and the indicated values of the pair (K_0, K_1). Figs. 3(e) and (f) take a different function of the form $F(\theta_0) = 1/(\theta_0^2 + 1)$ and different values of the pair (K_0, K_1) as indicated in the figures. In Figs. 3(a)–(d), the trajectories of the leader are the same as that in Fig. 1(a). Fig. 3(b) is an enlargement of the box in Fig. 3(a). The simulations in Figs. 3(a)–(e) all agree very well with the analytical results of Proposition that the particle members will move in the same manner if the directions of motion are neglected and that the weighted centroid tends to a fixed point for $K_1 < 0$. Moreover, noting $K_0/K_1 = 10 = N$ from the values of (K_0, K_1) in Fig. 3(e) and $F(\theta_0)/K_0 \to 0$ as $t \to +\infty$, the simulation in Fig. 3(e) verifies Remark 2.

Besides, some new features can also be seen from Figs. 3(a)–(d) and (f). Specifically, for those K_0 with small $|K_0|$, the particle members move along straight lines as shown in Figs. 3(a) and (c) in finite time slots. Fig. 3(d) shows that the

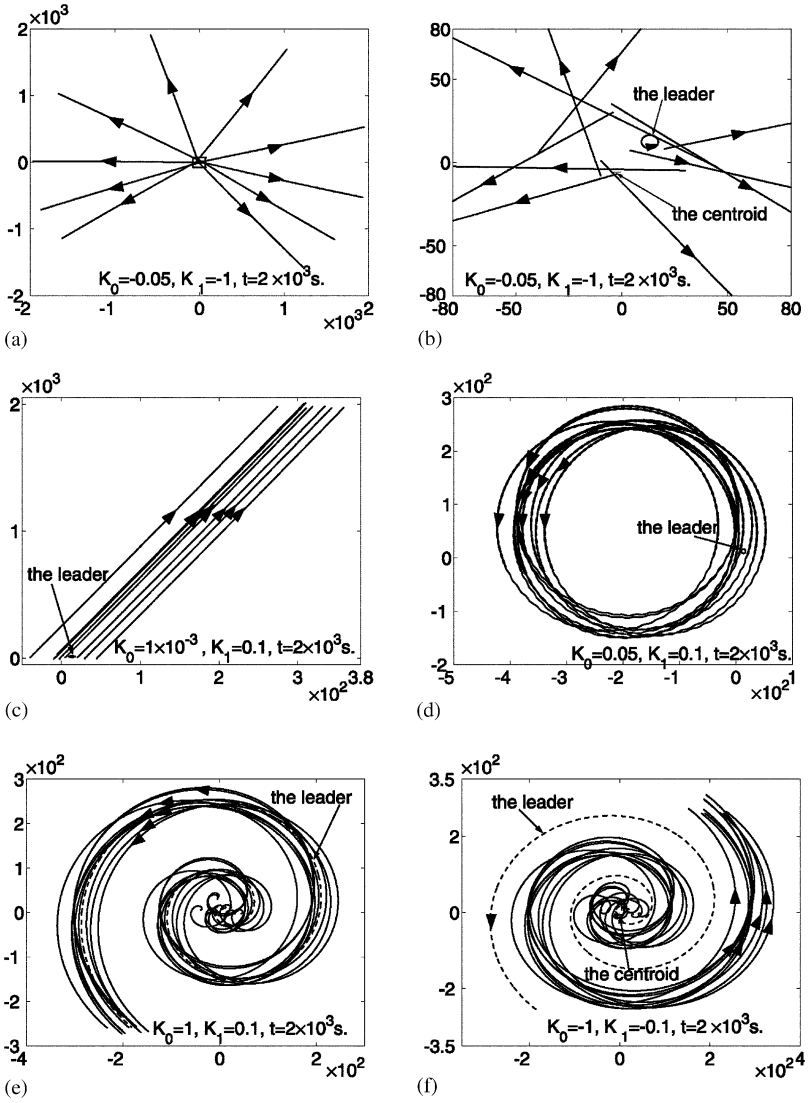

Fig. 3. Phase diagrams of the position dynamics of the particles with $F(\theta_0) = 0.25$ in (a)–(d) and $F(\theta_0) = 1/(\theta_0^2 + 1)$ in (e) and (f). The different values of pair (K_0, K_1) are indicated in the figures. In (a)–(f), the abscissa axis and the ordinate axis represent the first and the second components of the position vector r, respectively. The dashed lines in (e) and (f) indicate the trajectory of the leader.

members move in a similar manner to that the leader does when $K_1 > 0$ and $F(\theta_0)/K_0$ tends to a constant a with $|a| > 1$ as times increasing ($F(\theta_0)/K_0 \equiv 5$ for all time in Fig. 3(d)). Fig. 3(f) shows that the directions of the particle members are almost opposite to that of the leader for $K_1 < 0$ and $K_0/K_1 = N$

($K_0/K_1 = N = 10$ in Fig. 3(f)). Detailed analysis about these features are under investigation currently and will be presented elsewhere.

5. Conclusions

We have considered the collective dynamics of a motile particle group with a leader. Analytical study shows that the motion of all member particles depends on that of the leader and the coupling weights. In general, two types of collective motion will occur, depending on different ranges of the coupling weights among the members. One is that all members move in the same direction and the other is that all members move so that the weighted centroid of the group approaching a fixed position. In each case, all member particles will eventually move in the same manner if neglecting the directions of motion. Numerical simulations agree with the analytical results very well. The results of this paper show that it is possible to control the particle group by steering the motion of the leader. This is of practical interest in applications such as control of multi-robots or autonomous vehicles.

Acknowledgements

This work is supported by the National Natural Science Foundation of China (No. 60274001, No. 10372002) and the National Key Basic Research and Development Programme (No. 2002CB312200).

Appendix A

Proof of Assertion. First we prove (i). We only show $G_1 \geqslant 0$. The case of $G_2 \geqslant 0$ can be established similarly.

For $\gamma = 0$, from the expression of G_1, we have

$$G_1 = -\sum_{k=1}^{N} \cos(\psi_k - \Psi) - \frac{K_0}{K_1} \cos \Theta .$$

Since $\cos(\psi_k - \Psi) = \cos \psi_k \cos \Psi + \sin \psi_k \sin \Psi$, by (16)–(18), we get $G_1 = 0$.

For $0 < \gamma < 1$, since

$$\frac{\partial G_1}{\partial \gamma} = \sum_{k=1}^{N} \frac{1 - \cos^2(\psi_k - \Psi)}{[1 - \gamma \cos(\psi_k - \Psi)]^2} + 2\gamma \frac{K_0}{K_1}(1 + \cos \Theta) + \frac{K_0}{K_1} > 0$$

for all (Θ, Ψ, θ_0), then G_1 strictly increases in γ. Therefore $G_1 \geqslant 0$ for all $(\gamma, \Theta, \Psi, \theta_0)$ and the equality holds if and only if $\gamma = 0$.

Now we prove (ii). We only show the case of $K_1 > 0$. The case of $K_1 < 0$ can be done similarly. For $K_1 > 0$, we have

$$G_4 = \dot{v} - \gamma \sin \Theta F(\theta_0)$$
$$= \begin{cases} (2 - \gamma \sin \Theta)F(\theta_0) & \text{if } \theta_0 \in P2\,, \\ (-2 - \gamma \sin \Theta)F(\theta_0) & \text{if } \theta_0 \in P3\,, \\ (\theta_0 - \theta_0^* - 2 - \gamma \sin \Theta)F(\theta_0) & \text{if } \theta_0 \in P1(+)\,, \\ (\theta_0 - \theta_0^* + 2 - \gamma \sin \Theta)F(\theta_0) & \text{if } \theta_0 \in P1(-)\,. \end{cases}$$

According to Lemma 1, $G_4 > 0$ always holds as t is large enough. □

References

[1] C.M. Breder, Ecology 35 (1954) 361.
[2] K. Warburton, J. Lazarus, J. Theor. Biol. 150 (1991) 473.
[3] T. Vicsek, A. Czirók, E. Een-Jacob, I. Cohen, O. Shochet, Phys. Rev. Lett. 75 (1995) 1226.
[4] N. Shimoyama, K. Sugawa, T. Mizuguchi, Y. Hayakawa, M. Sano, Phys. Rev. Lett. 76 (1996) 3870.
[5] J. Toner, Y. Tu, Phys. Rev. E 58 (1998) 4828.
[6] J.D. Crawford, K.T.R. Davies, Physica D 125 (1999) 1.
[7] A. Czirók, M. Vicsek, T. Vicsek, Physica A 264 (1999) 299.
[8] A. Czirók, T. Vicsek, Physica A 281 (2000) 17.
[9] J.A. Acebrón, R. Spigler, Physica D 141 (2000) 65.
[10] H. Levine, W.-J. Rappel, Phys. Rev. E 63 (2001) 017101.
[11] R.E. Amritkar, S. Jalan, Physica A 321 (2003) 220.
[12] B. Liu, T. Chu, L. Wang, Z. Wang, Chinese Phys. Lett. 22 (2005) 254.
[13] N.E. Leonard, E. Fiorelli, Proceedings of the 40th IEEE Conference on Decision and Control, 2001, p. 2968.
[14] Y. Liu, K.M. Passino, M.M. Polycarpou, IEEE Trans. Automat. Control 48 (2003) 76.
[15] A. Jadbabaie, J. Lin, A.S. Morse, IEEE Trans. Automat. Control 48 (2003) 988.
[16] T. Chu, L. Wang, T. Chen, J. Control Theory Appl. 1 (2003) 77.
[17] T. Chu, L. Wang, S. Mu, Proceedings of the 16th International Symposium on Mathematical Theory of Networks and Systems (MTNS 2004), Paper ID: REG-345, Leuven, Belgium, July 2004.
[18] W. Wang, J.J.E. Slotine, Biol. Cybern. 92 (2005) 38.
[19] R. Sepulchre, D. Paley, N. Leonard, in: V.J. Kumar, N.E. Leonard, A.S. Morse (Eds.), Proceedings of the 2003 Block Island Workshop on Cooperative Control, Springer, Berlin, 2003.
[20] S. Watanabe, S. Strogatz, Physica D 74 (1994) 197.